

# INVESTIGATION ON THE THERMAL MANAGEMENT OF A HIGH POWER LED MODULE

V. VIGH<sup>1</sup>    L. KALMAR<sup>2</sup>    T. REGERT<sup>3</sup>

**Abstract:** *High power LED light sources operate mainly in the UV regime. Although the emitted light power is significant, a large amount of heat is generated as a side effect. The increasing temperature degrades the state of the electronic elements of the LED module and decreases the power of the emitted light. This paper discusses the results of the experimental and numerical modelling of the thermal processes inside a module containing a single LED element. Thermal characteristics were investigated for the case with and without forced cooling. Cooling was realized by using air flow induced by a fan. Parameters were identified that govern the main characteristics of the phenomenon.*

**Key words:** *high power UV LED, heat transfer, experiments, CFD.*

## 1. Introduction

The aim of the research presented in this paper is to investigate the thermal transfer process inside a high power LED module that produces light in the ultra violet (UV) regime. The LED light sources are continuously gaining popularity in lighting technology on almost all area of applications. The high light efficiency, i.e. the produced light quantity in lumens related to the input current, of LED light sources comparing to the conventional incandescent, halogen, sodium and fluorescent light puts them in a competitive position on the lighting market. An extensive analysis of the position of LED lights on the lighting market can be found in [2]. Low power LED lights operate at

input currents in the order of magnitude of 20 mA and their light efficiency is higher than that of the market-leading high pressure sodium lamps. Reference [3] discusses that the quantum efficiency of LED light sources takes its highest values in the UV domain (more than 60%) and is high also in the infrared (IR) domain (around 55%). However, it is poor in the visible light range. Although for low power LED lights the low quantum efficiency does not impose significant problems, high power LED lights encounter significant energy dissipation issues. For this reason, recently the high power LED sources are working in the UV domain. In recent applications the generated UV light is converted into the visible regime by using phosphor-based intensifiers. Although this

---

<sup>1</sup> Graduate student, Department of Fluid and Heat Engineering, University of Miskolc, Hungary.

<sup>2</sup> Associate Professor, Department of Fluid and Heat Engineering, University of Miskolc, Hungary.

<sup>3</sup> Senior Researcher, 39 Avenue Messidor, 1180 Brussels, Belgium.

conversion process is efficient, the resultant light remains always close to the blue tones.

The most significant problems related to LED light sources are: the high production cost which is still one order of magnitude higher than that of conventional light sources; the large current density (current related to the supplied surface area of the light source) that leads to intensive heating. When the temperature of a LED module increases the light efficiency decreases, thus cooling represents a major issue of these light sources. The cooling has to be sufficient to keep the temperature below 120 centigrade [1] and has to have low production and operation cost. Although for low power LED sources the level of heat generation is so low that natural convection based passive cooling is possible, in the case of high power LED sources forced cooling is indispensable.

In this paper the authors attempted to model the heating of a simplified LED module under forced cooling by means of a fan applying experimental and numerical simulation approaches. In the first part of the paper the experimental setup and the measurement technique is described. The following sections discuss the way of numerical modelling and the obtained results.

## 2. The Simplified LED Module

The LED light sources usually consist of a cluster of LEDs embedded in a special printed circuit board (PCB) which is called insulated metal substrate (IMS). The electronics and the interactions between the LEDs in the cluster are quite complex, thus for research purpose a PCB containing a single LED was constructed and is represented in Figure 1. The high power UV LED which is used for the measurements is the type of SL-V-U40AC. This is a SEMILEDS product, and all SemiLEDS UV

chips are made by using their own patented metal alloy MvpLED™ technology. This alloy provides the maximum heat transfer from the junction to the board or heat sink. These features along with the optical advantages facilitate designs using higher drive currents to maximize light density. SemiLEDS' patented and unique process uses a limited amount of sapphire, which can be recycled and reused multiple times, significantly reducing the carbon footprint. The reduced dependence on sapphire also removes a thermal management bottleneck while providing the most environmental friendly LED on the market [5].

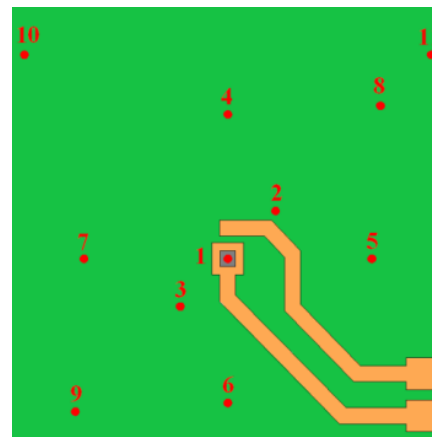


Fig. 1. *Schematic of the LED module with the measurement locations indicated by numbers*

The output power of the LED is: 75 mW - 380 mW producing light in the wavelength range of 375 nm - 435 nm. The efficiency of the UV LED was measured by using an Ulbricht sphere. Based on the measured data and the input power (3.4 V at 350 mA) the obtained efficiency of the light source is 9.66%.

## 3. Experimental Setup

Two test configurations were investigated: LED module with and without forced cooling. Figure 2 shows the LED module

held by clamps in horizontal position. The cooling was realized by using a processor cooling fan by producing a horizontal jet. The direction of the flow is from the top right to the bottom left in Figure 2. During the experiments the surface temperature of the LED and the PCB board was measured point wise.

The surface temperature of the PCB and the LED unit was measured by a small contact thermometer (Figure 2 right) of type OpSensTempSens which is based on optical sensing. Opsens' OTG-F fibre optic temperature sensor [6] is based on a GaAs electron-emissive element of size 150 $\mu$ m. Sampling frequency was 50 Hz, temperature resolution 0.1 K, response time of probe is 5 ms.

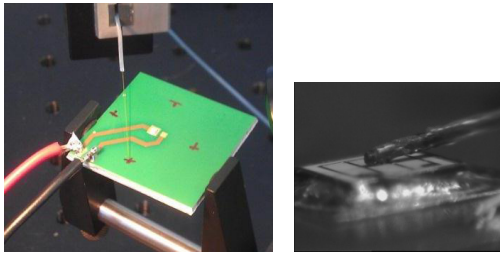


Fig. 2. Experimental setup (left) and a zoom on the contact heat sensor (right)

#### 4. Uncertainty Analysis of Experiments

The measurement uncertainty consists of the accuracy of the measured voltages, the measured current, the accuracy of the temperature measuring sensor and the corresponding processing electronics. For the forced cooling experiments also the velocity distribution of the air jet is affected by error. The measured voltage is indicated with a precision of 0.1 V, thus for the measured 3.4 V the relative error is 3% of the value. The current is indicated up to two digits, i.e. the error can be 0.01 A, which gives a relative error of 3% similarly to the measurement of voltages. From these errors the input power has a

resultant error of 0.05 W based on the theory of quadratic propagation of error, corresponding to a relative error of 4% of the measured power.

The temperature measurement accuracy is 0.1  $^{\circ}$ C which is determined by the signal processing unit, however a small change in the angle of the sensor might lead to a variation of 5  $^{\circ}$ C for the same temperature, thus at approximately 100  $^{\circ}$ C typical LED module temperature it means a relative error of 5%.

The air velocity measurement was based on the characteristic curve of the fan. The measurement error at the 3m/s air velocity is approximately 10% with this estimation method.

The last factor of the uncertainty analysis is the repeatability. In all the cases the measurements were repeated three times for each measurement point. It has been observed that the results did not differ from each other more than a maximum of 3% in the worst case.

## 5. Numerical Modelling

### 5.1. Governing equations

The LED module was modelled by the numerical code ANSYS-Fluent. This software makes it possible to compute the conjugate heat transfer from the LED into the PCB and into the surrounding environment. The principal purpose of the numerical analysis is the modelling of the heat transport inside the solid body. The energy transport equation has following form:

$$\frac{\partial}{\partial t}(\rho h) = \frac{\partial}{\partial x_i} \left( k_{tc} \frac{\partial T}{\partial x_i} \right) + S_h, \quad (1)$$

where:  $\rho$  [kg/m<sup>3</sup>] is the density;  $h = c_p T$  [J/kg] is the enthalpy;  $k_{tc}$  [W/mK] is the thermal conductivity;  $T$  [K] is the temperature

and  $S_h$  [J/m<sup>3</sup>] is volumetric heat source [4]. It can be seen in Equation (1) that the heat transport inside the solid body depends on material properties: density, heat capacity and thermal conductivity, and a volumetric heat source that is the LED in this case. All these parameters are charged with uncertainty, although the materials of the LED module are known, there are some unknown parameters, e.g. the thickness of protection lack layers applied on the surface. The uncertainty of the heat power of the LED, which acts the role of the volumetric heat source, has already been discussed in the previous section.

The LED module is surrounded by the ambient air, thus heat is transported from the solid region into the ambience. This heat transfer between the LED module and the ambience determines the equilibrium operating temperature of the LED module. Equation (1) is solved until the boundaries of the solid domain and the boundary conditions are computed from the solution of the energy equation of the ambient air.

The energy equation for the air is written as:

$$\begin{aligned} \frac{\partial}{\partial t}(\rho E) + \frac{\partial}{\partial x_j}(u_i(\rho E + p)) \\ = \frac{\partial}{\partial x_j} \left( k_{eff} \frac{\partial T}{\partial x_j} + u_i(\tau_{ij})_{eff} \right) + S_h, \end{aligned} \quad (2)$$

where:  $E$  [J/m<sup>3</sup>] is the total energy;  $k_{eff}$  is the effective thermal conductivity;  $T$  is the absolute temperature;  $S_h$  volumetric heat source and  $u_i(\tau_{ij})_{eff}$  is the power of the viscous forces. For the present case the power of the viscous forces can be neglected due to the very low velocity gradients and low velocities (3 m/s in the free stream for forced cooling). There is no volumetric heat source in the air. The only remaining term on the right hand side of Equation (2) is the heat conduction term that plays a critical role in the

determination of the equilibrium temperature distribution in the LED module. On the left hand side of Equation (2) the density of air is a function of temperature but as the pressure does not change reasonably, the density is independent on it. The second term of Equation (2) is the convective term for the energy that necessitates the solution for the equations of momentum of the air flow even in the case without forced cooling.

On the right hand side of Equation (2) the heat conduction term consists of the thermal conductivity of the air and the temperature gradient. Both of these terms are difficult to determine exactly. The temperature gradient has a critical role at the surface of the solid body, i.e. at the boundary of the LED module. The heat conduction coefficient is basically a material property, but in case of turbulent flow its value can be strongly affected by the turbulent heat transport. For this reason the thermal conductivity has the subscript “*eff*” that denotes the effective quantity, that is the resultant of the material property and the effect of turbulence.

## 5.2. Meshing and boundary conditions

For the computations a fully hexahedral but unstructured mesh was created containing 3.2 million cells. A mesh was made inside the solid LED module and in a box domain representing the surrounding air space.

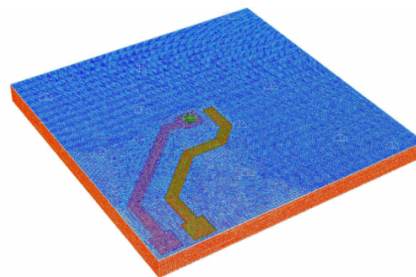


Fig. 3. Numerical mesh on the LED module

Due to the limited extension of the paper only the mesh on the LED module is shown in Figure 3 which indicates the characteristic mesh density.

The domain of the air has an inlet side where the velocity magnitude is prescribed. The opposite side to the inlet is the outlet surface where the average static pressure is prescribed. The sides of the domain are slip walls. The gravity is taken into account in the equations of the momentum.

The heat produced by the LED has been calculated to be 1050.2 mW. It has been prescribed as a volumetric source term.

The welding between the LED and the copper surface cannot be exactly characterized. The thickness has been assumed to be 0.1 mm and the thermal conductivity was determined based on experiments. The heating up transient of the LED module was measured and computed for the same conditions. The transient curve from the computation was tuned by adjusting the thermal conductivity of the welding and the heat capacity of the LED. The thermal conductivity influences mostly the equilibrium temperature of the LED, while the heat capacity of the LED affects the shape of the start-up transient.

The best result in the simulation for the welding's heat conductivity is 1.16 W/mK and heat capacity of 1200 J/kgK.

The correct heat capacity belongs to that of the material of the LED at 100 °C.

## 6. Results

### 6.1. Temperature evolution without forced cooling

The results of the experiments and the computations are shown together, thus they can be directly compared.

In Figure 4 one can observe the first part of the transient of the temperature from computations and from measurements for the first measurement point, which is the

one in the centre of the top surface of the LED.

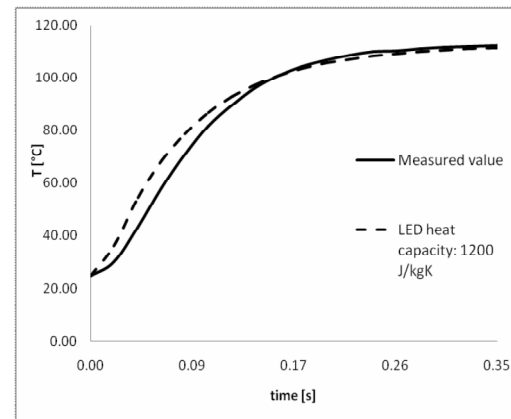


Fig. 4. Temperature transient for modified heat capacity. Case without forced cooling

This case is without forced cooling. Both numerical modelling and experiments show that the temperature increases from the ambient 25 °C to 115 °C in 0.2 seconds. It can be observed that after fine tuning the thermal conductivity and the heat capacity of the materials in the LED module, the numerical model and the experimental result are in a very good agreement. This part of the heating depends thus mainly on the heat conduction phenomenon interior in the LED module and there is only a weak effect of the interaction between the ambient air.

The long term behaviour of the temperature is represented in Figure 5. It can be seen that the increase of temperature is still in progress but the rate becomes slow. The curve computed from CFD shows a more significant increase in temperature for long term the measurement. This part of the heating process is mostly depending on the interaction between the LED module and the surrounding ambient air. Due to the lack of forced cooling, natural convection is generated that provides the transport of heat from the LED module to the ambience.

The natural convection process was not modelled by the CFD accurately, thus it can be concluded that as long term behaviour, the temperature of the LED module in the CFD model is increasing more than during the experiment. In the measurement points 2 and 3 the evolution of the temperature is significantly different from the one at measurement point 1, i.e. on the top of the LED.

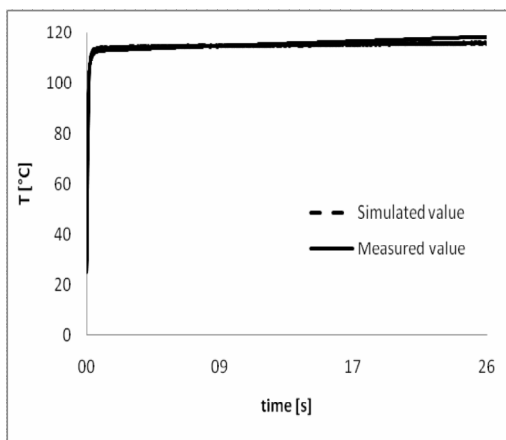


Fig. 5. Heat-up transient comparison on the centre of the top of the LED without forced cooling

In Figure 6 one can observe that the temperature increases almost linearly. Although the temperature of the LED achieves its equilibrium value in 0.4 seconds, the temperature of the PCB is still increasing slowly. It indicates also that the LED module has not arrived yet at its thermal equilibrium state with its ambience.

It can be seen that the numerical model predicts correctly the slope of the increase of temperature inside the PCB.

It can be concluded that the time scale of the heating of the LED is at least two orders of magnitude smaller than that of the PCB. This means that the LED can achieve high temperatures before the heat can be transported towards a cooling element that is usually on the opposite side of the PCB. The thermal equilibrium of the

LED is first established 0.4 seconds after the start-up. Another equilibrium temperature is expected after a sufficiently long time, when all the points of the hosting PCB reach also their thermal equilibrium.

The long term evolution of the temperature was determined by experiments and is shown for measurement point 1, i.e. the top of the LED.

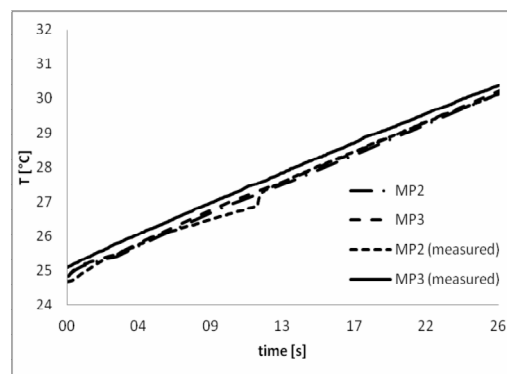


Fig. 6. Temperature evolution in measurement points 2 and 3

From this it was concluded that the equilibrium temperature establishes at around 8 minutes after the starting of the system. To see how it correlates with the temperature of the other surrounding points on the PCB, one can see their evolution in Figure 7.

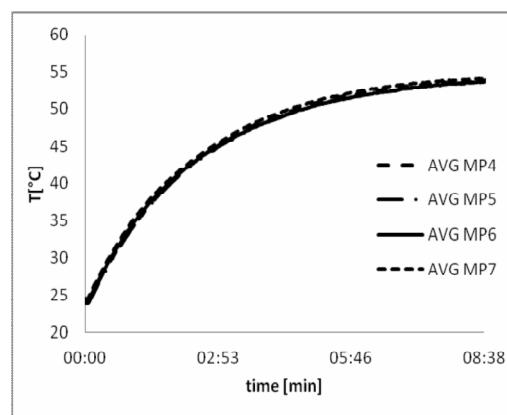


Fig. 7. Temperature evolution in the points of the PCB

It can be seen that the PCB, i.e. the bad conductor environment of the LED reaches its thermal equilibrium after around 8 minutes. In the numerical model such long period was not possible to be simulated, but the transient part has already shown that the agreement is good.

## 6.2. Temperature evolution with forced cooling

The forced cooling of the LED module was realized by using a processor cooling fan as described before. Due to the very approximate way of determination of the flow velocity of the fan, results from numerical simulation are not presented for this case.

It can be seen in Figure 8 that the temperature transient in the case when cooling is applied is very similar to the case without cooling. The temperature of the LED is approximately 5 degrees lower than without cooling.

It can be observed that the transient does not differ reasonably when forced cooling is applied. It indicates that the start-up transient is independent on the ambience.

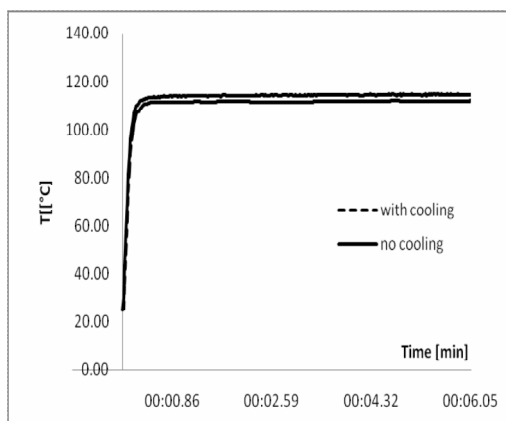


Fig. 8. Temperature evolution in measurement point 1 for the case of forced cooling compared to the case without forced cooling

The equilibrium temperature in the other measurement points is 19 degrees lower than in case of no cooling. The equilibrium sets in around 3 minutes as opposed to the 8 minutes of the non-cooled case.

## 7. Conclusions

A simplified LED module with a single LED element was investigated in terms of heat conduction inside the solid parts with simplified modelling of the interaction with the air ambience.

Measurements were carried out by using a contact optical sensor to obtain surface temperatures at various points of the LED module surface.

The configuration is modelled by means of numerical modelling of heat conduction inside the solid bodies by taking into account the ambient air on a simplified way. Two cases were analysed: one case with-, and another case without forced cooling. Forced cooling was realized by using a processor cooling fan.

The case without cooling was modelled by numerical simulation, while the forced cooling case was only investigated experimentally. The case without cooling showed that by correctly tuning the material properties of the LED module the transient and the final temperature of the LED module can be accurately simulated. It has been experienced that. The heat-up of the LED is two orders of magnitude faster than the surrounding PCB.

In case of forced cooling it has been found that the final temperature of the LED was 5 degrees lower than without cooling (natural convection only). The surface of the PCB arrived at a temperature, reasonably lower (19 degrees lower) than without cooling.

Although the PCB is cooled more when forced cooling was applied, it is still very slow comparing to the dynamics of the LED.

### Acknowledgements

The described work was carried out as part of the TÁMOP-4.2.1.B-10/2/KONV-2010-0001 project in the framework of the New Hungarian Development Plan. The realization of this project is supported by the European Union, co-financed by the European Social Fund.

### References

1. Arik, M., Becker, C., Weaver, S., Petroski, J.: *Thermal Management of LEDs: Package to System*. In: Third International Conference on Solid State Lighting, Ferguson, I.T, Narendran, N., et al. (Eds.), Bellingham, WA, Proceedings of the SPIE **5187** (2004), p. 64-75.
2. Craford, M.G.: *High Power LEDs for Solid State Lighting: Status, Trends, and Challenges*. In: Journal of Light Visual Environment **32** (2008) Issue 2, p. 58-62.
3. Krames, M.R., Shchekin, O.B., Mueller-Mach, R., Mueller, G.O., Zhou, L., Harbers, G., Crawford, M.G.: *Status and Future of High-Power Light Emitting Diodes for Solid-State Lighting*. In: Journal of Display and Technology **3** (2007) No. 2, p. 160-175.
4. ANSYS FLUENT 12.0: *Theory Guide*. ANSYS, Inc., 2009.
5. Web-reference on the high power UV-LED module: *Datasheet of SL-V-U40AC-UV-LED*: [http://semileds.com/system/files/SL-V\\_U40AC.pdf](http://semileds.com/system/files/SL-V_U40AC.pdf).
6. Web reference of temperature measurement sensor: *Datasheet of Opsens OTG-F sensor*. <http://www.opsens.com/pdf/products/OTG-F%20Rev1.5%20.pdf>.